ARTICLES

Great Himalayan earthquakes and the Tibetan plateau

Nicole Feldl[1] & Roger Bilham[1]

It has been assumed that Himalayan earthquakes are driven by the release of compressional strain accumulating close to the Greater Himalaya. However, elastic models of the Indo–Asian collision using recently imaged subsurface interface geometries suggest that a substantial fraction of the southernmost 500 kilometres of the Tibetan plateau participates in driving great ruptures. We show here that this Tibetan reservoir of elastic strain energy is drained in proportion to Himalayan rupture length, and that the consequent growth of slip and magnitude with rupture area, when compared to data from recent earthquakes, can be used to infer a ~500-year renewal time for these events. The elastic models also illuminate two puzzling features of plate boundary seismicity: how great earthquakes can re-rupture regions that have already ruptured in recent smaller earthquakes and how mega-earthquakes with greater than 20 metres slip may occur at millennia-long intervals, driven by residual strain following many centuries of smaller earthquakes.

Approximately one-half of India's 36–40 mm yr^{-1} northward motion is absorbed by convergence of the Himalaya, one-third in contraction of the Tibetan plateau, and the remainder is distributed between Tibet and Mongolia[1,2]. An important goal in Himalayan studies in the past decade has been to refine the Himalayan convergence rate, because this is responsible for the productivity of Himalayan earthquakes. It was anticipated that the uncertainty in the initial rate[3] would steadily decrease as more GPS (Global Positioning System) data became available. Although observed velocity uncertainties have decreased as expected, calculated convergence velocities range from 14 to 20 mm yr^{-1} (Table 1), with a preferred rate in central and eastern Nepal of 19 ± 2.5 mm yr^{-1} (ref. 4). In Supplementary Information we present additional GPS data from 16 points between 83° E and 87° E (Fig. 1) measured between 1991 and 2004 that further constrain the Himalayan convergence velocity.

We attempted initially to emulate the observed velocity field, as in previous studies, as the product of uniform creep on a planar dislocation beneath the plateau. This yielded a slip rate of 17 ± 1 mm yr^{-1} on a 6°, N12E dipping dislocation starting at 18 km depth, consistent with earlier results (Fig. 2), but we noted that our result (and its uncertainty) was influenced by the retention or rejection of GPS data 100–300 km north of the Himalayan foothills. No abrupt transition in surface velocity distinguishes the strain field above the process zone of Himalayan seismicity from that of the Tibetan plateau, whose 17×10^{-9} strain yr^{-1} north-northeast-directed contraction and east-southeast-directed extension have been interpreted as resulting from dynamic processes responsible for inelastic, permanent deformation of the plateau[5]. As the inclusion of more northerly GPS points biases interpretations of Himalayan convergence velocities to higher values, we adopted a different approach, where the Himalayan and Tibetan velocity fields are considered the surface manifestation of a single deformational process related to the slip of India beneath the plateau. Our study indicates that although the region of elastic strain accumulation and release is much broader than hitherto supposed, less than one-fifth of the strain currently accumulating in the southern 500 km of the plateau participates in the earthquake cycle.

A boundary element model for interseismic deformation

We assume that frictionless aseismic slip occurs between the descending Indian plate and the overlying Tibetan plateau in an elastic half-space. We simplified the Himalayan arc as a straight line, but used a receiver-function image of the descending Indian plate[6] as a 'cylindrical' subsurface starting geometry at its southern edge. We emulate this subsurface geometry with 14 contiguous, parallel, freely slipping boundary elements, with 64 elements along-strike[7] extending 500 km north of the Himalaya (Fig. 2). Element dimensions are 50 km along-strike, and 2 km wide near the Himalaya increasing to 180 km in the north. We imposed an appropriate convergence velocity on the northernmost element and an overall strain contraction rate at N10E to drive the model (see Supplementary Information). We then calculated the displacement on each segment needed to minimize stress in its vicinity[7–9] in response to these imposed loading conditions, and compared the resulting surface velocities with the observed horizontal and vertical velocities in the Himalaya and southern Tibet.

Although we tested several different northern boundaries for the model, we ultimately selected a northernmost driving segment whose southern edge lies close to where the plateau's surface converges with the Indian plate at a velocity of 21 mm yr^{-1}. This occurs ~550 km north of the frontal thrusts, near the Karakorum/Jiali fault system. The Himalaya advance over India at 14 mm yr^{-1} (refs 10 and 11) to 21 mm yr^{-1} (ref. 12), and the simplest assumption is that to sustain the highest rates of advance, at least 550 km of the southern plateau must participate in driving the Himalaya's southward advance. We determined that a surface convergence velocity of 21 mm yr^{-1} 550 km north of the frontal thrusts can be obtained by imposing a background strain of -4.8×10^{-8} yr^{-1}, and by driving the boundary element model with uniform slip of 25 mm yr^{-1} on a wide horizontal synthetic thrust fault 49 km below the plateau surface, whose southern edge lies 594 km north of the frontal thrusts. The driven dislocation is sufficiently far north to not introduce local gradients in the region of interest. To match the surface velocity field to GPS observations southward, we found it necessary to introduce minor adjustments to the depth and dip of the descending Indian plate near the transition from aseismic to seismic slip. Starting from the 'locking line' of our planar, uniform-slip model[3], the best fit was obtained by

[1]CIRES and Department of Geological Sciences, University of Colorado, Boulder, Colorado 80309, USA.

Table 1 | Himalayan convergence rates

Interval	Slip rate (mm yr^{-1})	Locking depth (km)	Dip (°)	Location	Source
1991–1995	20 ± 2 (18 ± 2*)	20 ± 4	4 ± 4	81–88° Nepal	Ref. 3
1991–1997	20 ± 1	15	3	Eastern Nepal	Ref. 36
	21 ± 2	25	4.5	Western Nepal	
	20 ± 1 (18 ± 2*)	18	5	Combined	
1991–1997	17.4 ± 0.7	9	0	Eastern Nepal	Ref. 37
	16.3 ± 0.4	12	1	Western Nepal	
1995–2000	19–20	17–21	9–10	Central Nepal	Ref. 38
	19	20–21	9–10	Western Nepal	
1995–2000	14 ± 1	15	6	Northwest India	Ref. 39
1997–2000	19 ± 3*	ND	ND	Ladakh	Ref. 40
1991–2000	17 ± 0.9	18.3	9.5	West Himalaya	Ref. 41
	12.2 ± 0.4	14.3	2.5	Central Himalaya	
	17.5–19	20.3	3	Eastern Himalaya	
1992–2004	19 ± 2.5	20.4	10.3	Central Nepal	Ref. 4
1992–2004	17 ± 2	18	9	Eastern Nepal	This study (planar models)[42]
	19 ± 3	18	6	Central Nepal	
	17 ± 1	18	9	Combined	
Holocene	21 ± 1.5	ND	ND	Central Nepal	Ref. 12
Holocene	≥14 ± 4	ND	ND	Kumaon Himal	Ref. 11
	≥12 ± 3	ND	ND	NW India	
Late Cenozoic	10–15*	ND	ND	73–87° Himalaya	Ref. 10
Late Cenozoic	18 ± 7*	ND	ND	73–87° Himalaya	Ref. 16

* Observed surface convergence rate, rather than estimated slip rate on dislocation. Current convergence rates are based largely on planar elastic dislocation models that derive a subsurface slip rate to emulate the surface velocities of GPS data. ND, not determined.

extending the region of aseismic slip 7.5 km further south, by reducing its depth from 18 to 15 km, and by increasing its dip from 9° to 22° N. These geometrical adjustments are permitted by current uncertainties in the geometry of the interface[6], and the probable presence of a structural ramp beneath the Greater Himalaya. A feature of these elastic models is that they predict a broad region where the basal slip-velocity reduces to zero at the tip of the dislocation beneath and south of the Greater Himalaya. Finite element models that have included rock rheology also report a wide region where slip reduces to zero[13]. The termination of interseismic slip 83 km north of the frontal thrusts reduces the width of Himalayan ruptures from previous estimates (90–110 km) unless additional coseismic slip extends downdip during earthquakes into the region of interseismic slip. Downdip slip here is essential either as coseismic slip or afterslip to eliminate the accumulation of a permanent slip deficit. We later compute its numerical value and spatial distribution.

The dip required by the model beneath the Greater Himalaya is in good agreement with the average dip of moderate earthquakes occurring there[14–16]. Whereas the fit to the horizontal GPS data and vertical levelling data[17] is satisfactory, predicted vertical deformation is broader than that associated with planar, uniform slip models[3]. Vertical GPS data in southern Tibet are insufficiently precise at present to test the predicted width of this vertical uplift[18,19]. In contrast to the sensitivity of the model to the geometry of the descending Indian plate at depths shallower than 20 km, tests showed that the misfit in central Tibet is largely insensitive to the depth of the interface further north.

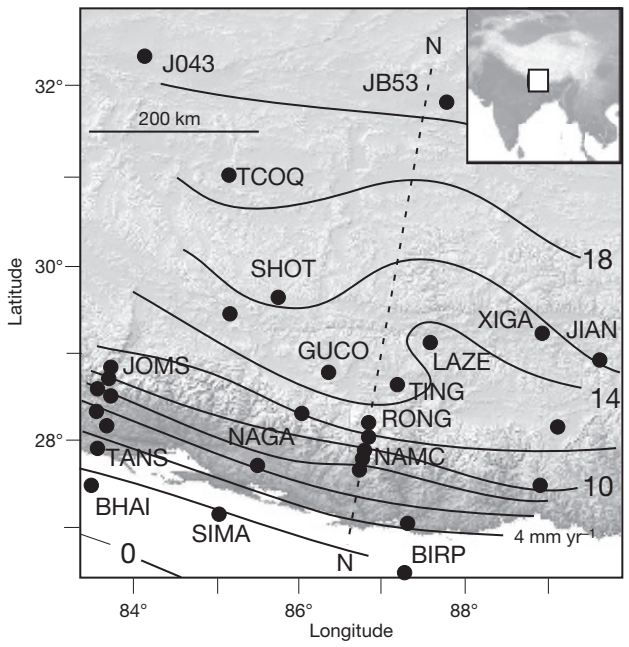

Figure 1 | The southern Tibetan plateau and Himalaya. Filled circles, GPS points; contours, the N10E GPS velocity field relative to India fixed; dashed line, the N10E velocity profile shown in Fig. 2. Inset, location of study area.

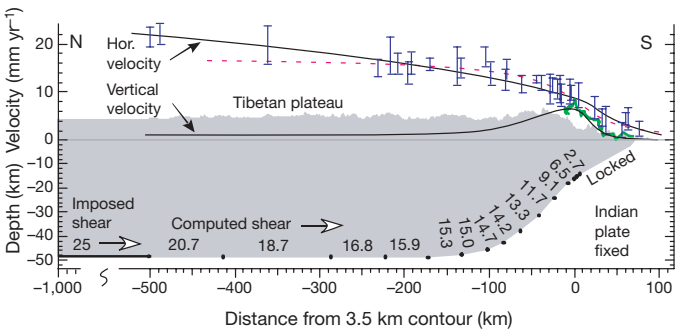

Figure 2 | Observed and synthetic present-day velocity fields for the southern Tibetan plateau. Observed fields are shown blue (horizontal GPS) and green (spirit-levelling[17]); synthetic fields are shown black; error bars are 1σ. Calculated interseismic segment velocities (mm yr^{-1}) and the geometry of freely slipping boundary elements are indicated at the base of plateau. The model is driven by a thrust fault in the north at 25 mm yr^{-1} (sense of shear indicated by arrow), and a background strain contraction rate of 4.8×10^{-8} yr^{-1} (corresponding to the mean strain rate between −500 km and the locking line). Dots indicate segment boundaries. The red dashed line shows the predicted velocity from the best-fitting planar dislocation model (see Supplementary Information). The grey shaded region represents the subsurface geometry and topography of the plateau.

Table 2 | Himalayan earthquake magnitude and slip versus rupture length

Length (km)	10	20	40	60	80	100	150	200	300	400	600	1200	2000
M_w restrained	*6.71*	*6.95*	*7.41*	*7.71*	*7.99*	*8.1*	*8.26*	*8.37*	*8.49*	*8.59*	*8.71*	*8.86*	*9.06*
Max. slip (m)	*3.41*	*3.81*	*4.55*	*5.64*	*6.98*	*7.78*	*8.76*	*9.05*	*9.12*	*9.11*	*9.11*	*9.12*	*9.12*
Ave slip (m)	*2.12*	*2.43*	*3.02*	*3.75*	*4.63*	*5.31*	*6.31*	*6.8*	*7.15*	*7.36*	*7.44*	*7.48*	*7.48*
M_w unrestrained	6.72	6.96	7.42	7.77	8.05	8.18	8.36	8.5	8.66	8.77	8.9	9.13	9.28
Max slip (m)	3.42	3.85	4.74	7.43	9.12	10.86	13.14	15.31	17.42	18.57	19.72	20.91	21.05
Ave. slip (m)	2.24	2.47	3.11	4.55	5.5	6.75	8.51	10.34	12.07	13.05	13.86	15.04	15.41
Max. 0–50 km N	0.01	0.05	0.11	1.12	1.57	2.29	3.65	5.69	8.22	9.83	11.52	13.2	13.4
Max. 50–200 km N	0	0.03	0.06	0.31	0.49	0.74	1.24	2.1	3.43	4.5	5.86	7.47	7.68

Calculations for 1,000 yr of Indo/Asian convergence at current rate. A halving in strain accumulation time (500 yr), consistent with ruptures in the past century (Fig. 4), halves the potential slip and reduces magnitudes by 0.2 M_w units. For ruptures where length $L \geq 80$ km, width w is 83 km. For ruptures where $L < 80$ km, areas are equidimensional. The first three rows in italics indicate Himalayan slip assuming that there is no coseismic slip beneath the plateau (restrained slip). The remaining five rows indicate coseismic or postseismic slip assuming that the plateau responds to the sudden southward shift in boundary conditions following Himalayan earthquakes (unrestrained slip). Unrestrained M_w magnitudes in row 4 are calculated assuming all slip is seismic. These end-member solutions form the upper and lower bounds of areas plotted in Fig. 4a and b. Maximum unrestrained trans-Himalayan coseismic displacements 0–50 km north of each rupture, and 50–200 km north of each rupture, are indicated in the last two rows.

Rupture length, earthquake magnitude and recurrence interval

We next examined the efficiency with which distributed strain stored within the southern plateau can be delivered to Himalayan earthquakes. Assuming that rupture occurs between the southernmost tip of interseismic slip beneath the plateau and the frontal thrusts, and that the slip is frictionless, the length of Himalayan ruptures determines the slip and consequently the magnitude of the earthquake. For example, if interseismic displacements were to accumulate in our model for 1,000 yr at present rates, the Himalaya would slip 21 m, were it to do so in a single massive earthquake. Assuming a rupture width of 83 km and length of 1,800 km, the moment magnitude of this improbably large earthquake would be $M_w = 9.2$ (Table 2). A 500-yr recurrence interval, however, would result in half the slip and a $M_w = 9.0$ earthquake. To calculate the slip on shorter rupture lengths, we incremented the slip velocities of our best-fitting interseismic boundary element model by 1,000 yr, and emulated an earthquake rupture by adding a freely slipping rectangular dislocation to its southernmost edge (Fig. 3). This additional rectangular region represents rupture of the Himalayan decollement, and was modelled as a 5×10 matrix of freely slipping elements, whose integrated slip and area were used to calculate M_w. In these synthetic earthquakes, we determined both the maximum and mean slip on the earthquake rupture, as well as the change of slip and strain beneath southern Tibet resulting from the occurrence of each Himalayan rupture (Table 2).

Two end-member models were considered. In the first, we calculate Himalayan slip assuming that no slip beneath the plateau accompanies rupture—that is, coseismic slip at the northern edge of the earthquake ceases abruptly at the southern edge of the region of aseismic slip. In the second, we calculate the combined change in slip on the earthquake rupture and beneath the plateau—that is, the northern edge of the earthquake rupture is unrestrained and is driven by strain relaxation in the southern plateau. This unrestrained additional slip more than doubles the maximum slip available to drive the frontal thrusts. This downdip slip presumably occurs as afterslip resulting in rate changes following rupture[20]: however, the 6 June 1505 earthquake[21] with its inferred 600-km-long rupture length was accompanied by substantial accelerations in southern Tibet, consistent with some of this downdip slip occurring co-seismically. Our results (Table 2 and Fig. 4) demonstrate that, as expected, for earthquakes with rupture lengths shorter than the width of the Himalaya, magnitude scales with area, whereas those longer than 90 km scale with length. Similar observed, and synthetic, scaling relations have been reported for transform faults[22–24]. Ruptures shorter than ~150 km leave strain in southern Tibet largely untapped, whereas longer ruptures drain this energy, resulting in larger slip both in the region of coseismic rupture and as increased slip downdip from the rupture beneath the plateau (Figs 4, 5).

The renewal time for Himalayan earthquakes is unknown, because no large earthquakes have recurred repeatedly in the historical record. The slip released in recent earthquakes compared to present-day Himalayan convergence rates suggests that the renewal time is of the order of 300–1,000 yr. This estimate can be improved using the synthetic scaling law depicted in Fig. 4, by selecting a renewal time consistent with M_w versus rupture-length data from recent earthquakes. Only for the 2005 Kashmir earthquake are slip and geometry well constrained, but the convergence rate in western Kashmir is lower, and the geometry of its rupture steeper, than for earthquakes we consider here. Such data as are available are consistent with a recurrence interval of ~500 yr, and suggest that recent ruptures best fit the restrained rupture model (the lower bound of the envelopes in Fig. 4).

Whereas the maximum slip in recent earthquakes is consistent with maximum slip predicted in synthetic earthquakes with a 500-yr return time, trench excavations of surface ruptures of medieval earthquakes record slip that would require ≥1,000 yr of strain accumulation[25,26]. Minimum rupture lengths only are available for these earthquakes, but our models imply that they ruptured much longer fault planes than

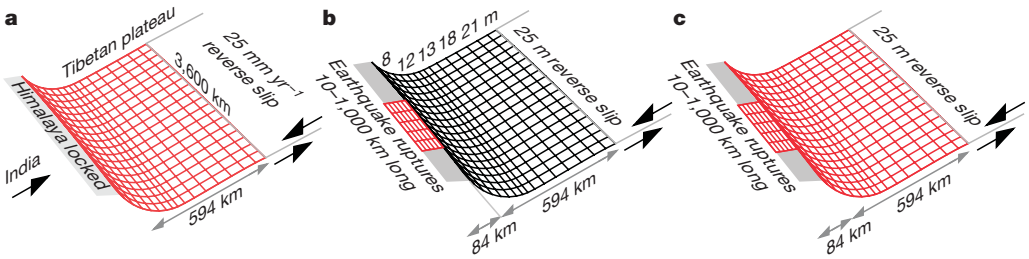

Figure 3 | Boundary element meshes used to derive synthetic slip. Red elements slip freely in response to imposed slip. **a**, Interseismic velocities calculated by driving 3,450 freely slipping elements with southerly geometry adjusted to emulate observed surface GPS data. **b**, Restrained coseismic slip. Velocities from **a** are used to derive displacements whose resulting strain field drives ruptures of different lengths in the Himalaya (Table 2). The displacements shown correspond to a millennium of slip at current rates. **c**, Slip beneath the Himalaya changes the boundary conditions in the southern plateau, causing additional slip both on the main rupture and beneath the plateau. When fully expressed, this unrestrained slip represents maximum afterslip (Table 2 and Fig. 4).

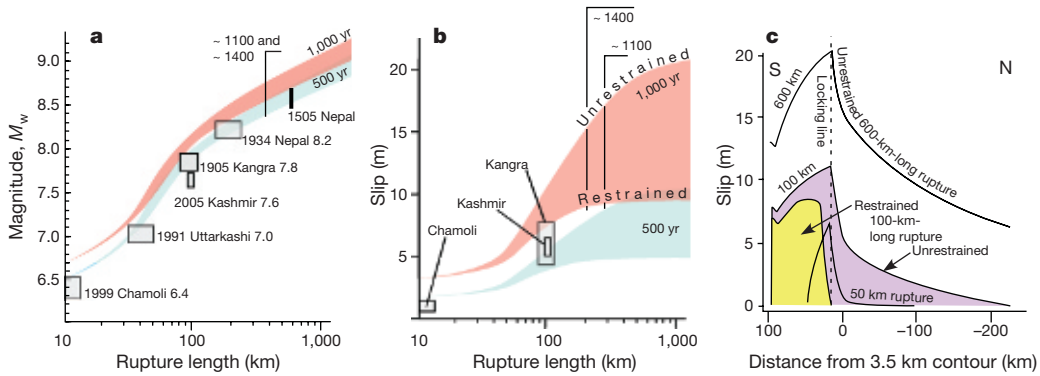

Figure 4 | Synthetic scaling laws for Himalayan earthquakes. Pink areas in **a** and **b** represent predictions for 1,000-yr intervals between earthquakes; blue areas represent predictions for 500 yr.The upper and lower bounds of these shaded areas correspond to restrained coseismic slip, and unrestrained slip, respectively. Restrained slip occurs coseismically when the interface below the plateau remains locked during the earthquake. **a**, M_w versus rupture-length curves suggest observed earthquakes recur after ~500-yr intervals. **b**, Envelopes indicate minimum slip (no plateau afterslip) and maximum slip (full strain release) for Himalayan ruptures. Maximum slip in medieval earthquakes requires >1,000 yr strain accumulation intervals. Open boxes are minimum estimates for historical ruptures (>300 km for about AD 1100 (ref. 26) and >200 km about AD 1400 (ref. 25). The eastern Nepal earthquake of 6 June 1505 is believed to have ruptured 600 km along the arc[21] and its recurrence now would release ~9 m of slip in a $M_w \approx 8.6$ earthquake (vertical bar in **a**). **c**, Maximum fault slip versus north/south distance as a function of rupture length. Yellow indicates restrained coseismic slip for a 100-km-long rupture (no slip north of the locking line): violet indicates complete unrestrained strain release (frictionless slip beneath the plateau). The kink in the south is caused by the surface rupture of the steeply dipping Main Boundary Fault.

recent earthquakes (Table 2). A possible explanation for these observations of large slip is that they are amplified locally by the dynamics of rupture[23,27], but it is more probable that long ruptures (megaquakes) at infrequent intervals are essential to occasionally reduce residual elastic strain accumulating in the southern plateau that has been left by previous smaller earthquakes. The past 500 yr, for example, are characterized by earthquakes with rupture lengths <300 km that have inefficiently reduced cumulative elastic strain.

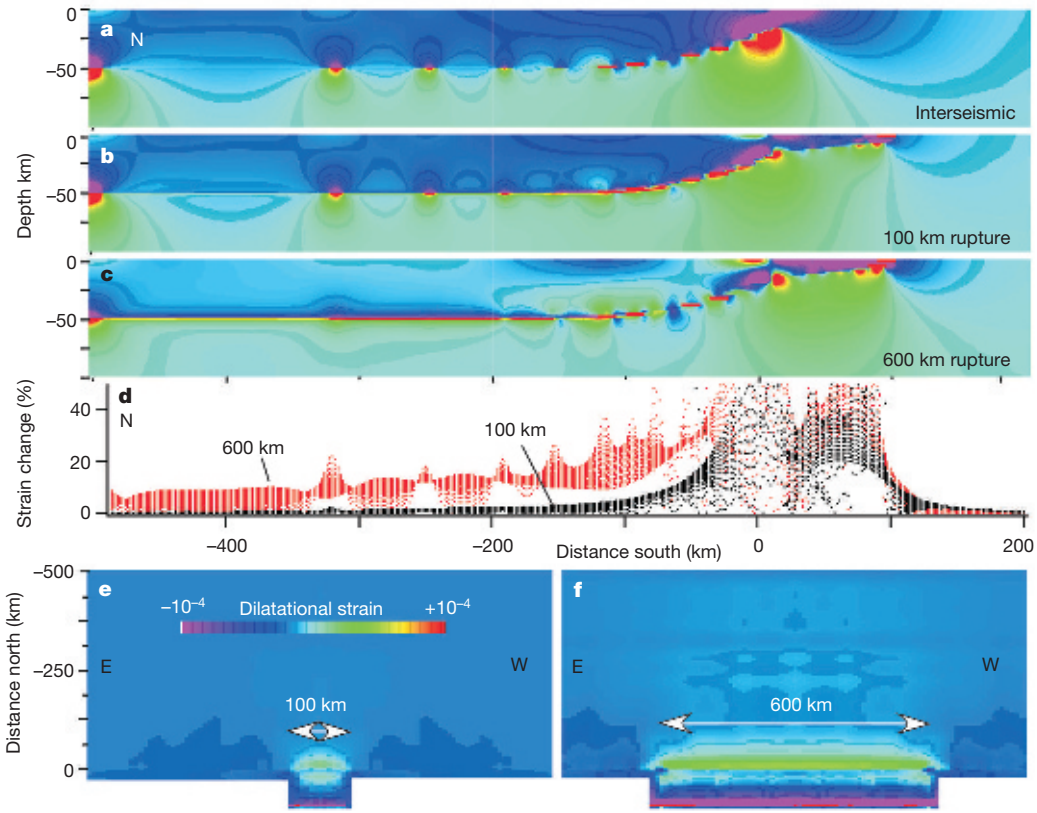

Figure 5 | Unrestrained strain changes in the southern Tibetan plateau generated by synthetic earthquakes with 100-km-long ($8 < M_w < 8.2$) and 600-km-long ($8.4 < M_w < 8.6$) ruptures. Shown are cross-sections (**a**–**d**) and map views (**e**, **f**). **a**, Pre-seismic dilational strain associated with 1,000 yr of strain accumulation at the current rate. **b**, **c**, Coseismic changes caused by earthquakes with 100-km (**b**) and 600 km (**c**) rupture lengths (**e** and **f** are respective map views of surface strain changes). **d**, Calculated percentage strain changes in the uppermost 40 km of the plateau for these two lengths of rupture. Cusps and strain concentrations in each panel are artefacts caused by junctions between boundary elements (see Fig. 2). Cross-sections **a**–**c** sample the centre of each rupture, but **d** samples all points shallower than 45 km throughout a ±500-km east–west length of the southern plateau. Colour coding for dilatational strain in **a**–**c** and **f** shown in **e**.

Seismic gaps versus failures in seismic gap theory

We note that our inferred renewal time applies to earthquakes of all magnitudes, which is an apparent departure from the predictions of seismic gap theory. Seismic gaps are unruptured segments of a plate boundary that slip eventually in great earthquakes. Their rupture results in an earthquake whose magnitude is characteristically proportional to the cumulative plate boundary displacement since their previous rupture. Our models suggest that once a critical strain has been attained, its release by a $M_w < 7$ or a $M_w > 9$ earthquake depends only on the length of the rupture, the growth of which in the Himalaya is presumably impeded by the presence of along-arc asperities[28]. Insufficient earthquakes are known in the Himalaya to determine whether successive earthquakes rupture similar areas.

A second apparent departure from seismic gap theory is that our model demonstrates that a major earthquake can be followed by a great earthquake in the same location, sooner than anticipated from considerations of renewal time from plate convergence rates. Such behaviour is manifest in other convergence zones: in Chile[29] and in the 2004 Sumatra/Andaman earthquake[30]. Himalayan $M_w < 8$ earthquakes drain negligible elastic energy from southern Tibet compared to those where $M_w > 8$. This can explain, for example, why the 1833 $M_w = 7.8$ Nepal earthquake was followed by the 1934 $M_w = 8.2$ Bihar/Nepal earthquake in approximately the same area after only 101 yr (ref. 31). It also implies that the 1905 Kangra earthquake region, previously considered a region reprieved from an imminent damaging earthquake, could today host one of larger magnitude[32].

That the elastic cycle accompanying Himalayan earthquakes must modulate the stresses that drive the long term flow behaviour of the plateau has never been questioned, but its influence in the southernmost 500 km of the plateau is unexpected. The elastic model we propose for the Tibetan plateau is a one-parameter model, driven by hypothetical reverse slip less than 500 km north of the Himalaya. This remote driving condition is not an unique requirement of the model, and similar results can be obtained using more northerly boundary conditions driven at higher rates, indicating that our conclusions are unaffected by elastic conditions in central and northern Tibet. Our traction-free lower boundary conditions at the base of the plateau are common to both dynamic[33] and kinematic models proposed for the Tibetan plateau[34], but unlike previous studies that incorporate realistic subsurface interface geometry, we incorporate no depth-dependent rheology, nor rate-dependent friction laws. Although the models may be refined further, the implications for earthquake scaling laws in the Himalaya are unlikely to change significantly.

The dynamic deformation of the Tibetan plateau is driven by the same forces that drive earthquakes in the Himalaya, and it is thus of some interest to estimate what fraction of present day strain accumulation in the plateau participates in the elastic earthquake cycle. Accordingly, we calculated the percentage of elastic strain released in the uppermost 40 km on a 2-km three-dimensional grid spacing throughout the southern plateau (Fig. 5d). Strain changes exceed 40% within 120 km of the Himalayan front but fall rapidly northward. For 100-km- and 600-km-long ruptures, dilatational strain changes average less than 10% and 20%, respectively, hence most of the observed interseismic strain remains to drive the dynamics and kinematics of the plateau.

The absence of surface ruptures for nineteenth- and twentieth-century central Himalayan earthquakes[35] suggests that their rupture lengths may have been atypically short (<200 km), and their slip correspondingly low. According to our models, the lengths of ruptures in about 1100 and 1400, which did rupture the surface, may have exceeded 400 km, with moment magnitudes exceeding $M_w = 8.6$. A ~500-yr recurrence interval for Himalayan earthquakes suggests that the western Himalaya (last mega-event in about 1400), the central Himalayan seismic gap (1505) and eastern Nepal (1100) are now sufficiently mature to sustain renewed rupture, but that the large observed slips (>20 m) of the first and last of these may require the elapse of a further five centuries before they repeat with equal severity.

Received 26 January; accepted 25 August 2006.

1. DeMets, C., Gordon, R. G., Argus, D. F. & Stein, S. Effect of recent revisions to the geomagnetic reversal time scale on estimates of current plate motions. *Geophys. Res. Lett.* **21,** 2191–2194 (1994).
2. Zhang, P. *et al.* Continuous deformation of the Tibetan Plateau from global positioning system data. *Geology* **32,** 809–812 (2004).
3. Bilham, R., Larson, K., Freymueller, J., Project Idylhim members. GPS measurements of present-day convergence across the Nepal Himalaya. *Nature* **386,** 61–64 (1997).
4. Bettinelli, P. *et al.* Plate motion of India and interseismic strain in the Nepal Himlayan from GPS and DORIS measurements. *J. Geod.* doi:10.1007/s00190-006-0030-3 (published online 8 March, 2006).
5. Houseman, G. & England, P. Crustal thickening versus lateral expulsion in the India-Asia continental collision. *J. Geophys. Res.* **98,** 12233–12249 (1993).
6. Schulte-Pelkum, V. *et al.* Imaging the Indian Subcontinent beneath the Himalaya. *Nature* **435,** 1222–1225 (2005).
7. Crouch, S. L. & Starfield, A. M. *Boundary Element Methods in Solid Mechanics* (Allen Unwin, London, 1983).
8. Gomberg, J. & Ellis, M. Topography and tectonics of the central New Madrid seismic zone: Results of numerical experiments using a three-dimensional boundary-element program. *J. Geophys. Res.* **99,** 20299–20310 (1994).
9. Okada, Y. Internal deformation due to shear and tensile faults in a half-space. *Bull. Seismol. Soc. Am.* **82,** 1018–1040 (1992).
10. Lyon-Caen, H. & Molnar, P. Gravity anomalies, flexure of the Indian plate, and the structure, support and evolution of the Himalaya and Ganga Basin. *Tectonics* **4,** 513–538 (1985).
11. Wesnousky, S. G., Kumar, S., Mohindra, R. & Thakur, V. C. Uplift and convergence along the Himalayan Frontal Thrust of India. *Tectonics* **18,** 967–976 (1999).
12. Lave, J. & Avouac, J. P. Active folding of fluvial terraces across the Siwaliks Hills, Himalayas of central Nepal. *J. Geophys. Res.* **105,** 5735–5770 (2000).
13. Cattin, R. & Avouac, J. P. Modelling mountain building, the seismic cycle in the Himalaya of Nepal. *J. Geophys. Res.* **105,** 13389–13407 (2000).
14. Molnar, P. & Lyon-Caen, H. Fault plane solutions of earthquakes and active tectonics of the Tibetan Plateau and its margins. *Geophys. J. Int.* **99,** 123–153 (1989).
15. Chen, W-P. & Molnar, P. Seismic moments of major earthquakes and the average rate of slip in Central Asia. *J. Geophys. Res.* **82,** 2945–2969 (1977).
16. Molnar, P. A review of geophysical constraints on the deep structure of the Tibetan Plateau, the Himalaya, and the Karakorum and their tectonic implications. *Phil. Trans. R. Soc. Lond. A* **326,** 33–88 (1988).
17. Jackson, M. & Bilham, R. Constraints on Himalayan deformation inferred from vertical velocity fields in Nepal and Tibet. *J. Geophys. Res.* **99,** 13897–13912 (1994).
18. Chen, J. Y. & Zhang, J. On the crustal movement in Quomolongma Feng and its adjacent area. *Acta Geophys. Sinica* **39,** 67–78 (1996).
19. Xu, C., Jungnan Liu, W. J. & Chuang, S. GPS measurements of present day uplift in Southern Tibet. *Earth Planets Space* **52,** 735–739 (2000).
20. Perfettini, H. & Avouac, J. P. Stress transfer and strain rate variations during the seismic cycle. *J. Geophys. Res.* **109,** doi:10.1029/2003JB002917 (2004).
21. Ambraseys, N. & Jackson, D. A note on early earthquakes in northern India and southern Tibet. *Curr. Sci.* **84,** 570–582 (2003).
22. Wells, D. L. & Coppersmith, K. L. New empirical relationships among magnitude, rupture width, rupture area, and surface displacement. *Bull. Seismol. Soc. Am.* **84,** 974–1002 (1994).
23. Shaw, B. E. & Scholz, C. H. Slip-length scaling in large earthquakes: Observations and theory and implications for earthquake physics. *Geophys. Res. Lett.* **28,** 2995–2998 (2001).
24. Bodin, P. & Bilham, R. 3-D geometry at transform plate boundaries: Implications for seismic rupture. *Geophys. Res. Lett.* **21,** 2523–2526 (1994).
25. Kumar, S. *et al.* Paleoseismic evidence of great surface rupture earthquakes along the Indian Himalaya. *J. Geophys. Res.* **111,** B03304, doi:10.1029/2004JB003309 (2006).
26. Lave, J. *et al.* Evidence for a great medieval earthquake (~1100 A.D.) in the Central Himalayas, Nepal. *Science* **307,** 1302–1305 (2005).
27. Brune, J. N., Brown, S. & Johnson, P. A. Rupture mechanism and interface separation in foam rubber models of earthquakes: a possible solution to the heat flow paradox and the paradox of large overthrusts. *Tectonophysics* **218,** 59–67 (1993).
28. Bollinger, L., Avouac, J. P., Cattin, R. & Pandey, M. R. Stress buildup in the Himalaya. *J. Geophys. Res.* **109,** doi:10.1029/2003JB002911 (2004).
29. Cisternas, M. *et al.* Predecessors of the giant 1960 Chile earthquake. *Nature* **437,** 404–407 (2005).
30. Bilham, R., Engdahl, E. R., Feldl, N. & Satyabala, S. P. Partial and complete rupture of the Indo-Andaman plate boundary 1847–2004. *Seismol. Res. Lett.* **76,** 299–311 (2005).
31. Bilham, R. Earthquakes in India and the Himalaya: Tectonics, geodesy, and history. *Ann. Geophys.* **74,** 839–858 (2004).
32. Bilham, R. & Wallace, K. Future Mw>8 earthquakes in the Himalaya: Implications from the 26 Dec 2004 Mw=9.0 earthquake on India's eastern plate margin. *Geol. Surv. India Spec. Publ.* **85,** 1–14 (2005).

33. England, P. & Molnar, P. Active deformation of Asia: From kinematics to dynamics. *Science* **278,** 647–650 (1997).
34. Tapponnier, P. *et al.* Oblique stepwise rise and growth of the Tibet Plateau. *Science* **294,** 1671–1677 (2001).
35. Bilham, R. & Ambraseys, N. Apparent Himalayan slip deficit from the summation of seismic moments for Himalayan earthquakes, 1500–2000. *Curr. Sci.* **88,** 1658–1663 (2005).
36. Larson, K., Burgmann, R., Bilham, R. & Freymueller, J. Kinematics of the India-Eurasia collision zone from GPS measurements. *J. Geophys. Res.* **104,** 1077–1093 (1999).
37. Burgmann, R., Larson, K. & Bilham, R. Model inversion of GPS and leveling measurements across the Himalaya: Implications for earthquake hazards and future geodetic networks. *Himal. Geol.* **20,** 59–72 (1999).
38. Jouanne, F. *et al.* Current shortening across the Himalayas of Nepal. *Geophys. J. Int.* **157,** 1–14 (2004).
39. Banerjee, P. & Burgmann, R. Convergence across the northwest Himalaya from GPS measurements. *Geophys. Res. Lett.* **29,** 31–34 (2002).
40. Jade, S. *et al.* GPS measurements from the Ladakh Himalaya, India: Preliminary tests of plate-like or continuous deformation in Tibet. *Geol. Soc. Am. Bull.* **116,** 1385–1391 (2004).
41. Chen, Q. *et al.* Spatially variable extension in southern Tibet based on GPS measurements. *J. Geophys. Res.* **109,** B09401, doi:10.1029/2002JB002350 (2004).
42. Feldl, N. *Crustal Deformation Across the Himalaya of Central and Eastern Nepal.* MSc thesis, Univ. Colorado (2005).

Supplementary Information is linked to the online version of the paper at www.nature.com/nature.

Acknowledgements Discussions with P. Bodin, J. Gomberg, G. King, P. Molnar and W. Szeliga, and written comments from S. Wesnousky, J.-P. Avouac and J. Freymueller, have improved the manuscript. This paper is based upon work supported by the National Science Foundation.

Author Contributions The 2003/4 GPS observations in Nepal were conducted by N.F. and R.B., and the planar dislocation models presented here formed the focus of N.F.'s MSc thesis at the University of Colorado.

Author Information Raw GPS data are available from UNAVCO (http://www.unavco.org/). Reprints and permissions information is available at www.nature.com/reprints. The authors declare no competing financial interests. Correspondence and requests for materials should be addressed to R.B. (bilham@colorado.edu.)